



## OPEN PRAME expression in fibrosarcomatous dermatofibrosarcoma protuberans

Toshio Ichiki<sup>1,2</sup>, Takamichi Ito<sup>2</sup>, Sakura Shiraishi<sup>1,3</sup>, Yasuharu Nakashima<sup>3</sup>, Takeshi Nakahara<sup>2</sup> & Yoshinao Oda<sup>1</sup>✉

PRAME (PReferentially expressed Antigen in MELanoma) was first identified as a malignant melanoma-specific antigen. Recently, a few cases of fibrosarcomatous dermatofibrosarcoma protuberans (FS-DFSP) were shown to have positivity for PRAME, while conventional dermatofibrosarcoma protuberans (C-DFSP) was negative. Because PRAME may be of diagnostic utility in FS-DFSP and is raising expectations as a new immunotherapy target, we examined the positivity of PRAME in FS-DFSP. Twenty-one cases of FS-DFSP and age/sex/location-matched cases of C-DFSP as a control group were examined by immunohistochemistry for CD34 and PRAME. The results were then evaluated by H-score, which was objectively and semi-quantitatively calculated using the open-source bioimaging analysis software QuPath. The results revealed that the PRAME H-score in FS-DFSP was significantly higher than that in C-DFSP ( $p = 0.0137$ ). As for CD34, the H-score in FS-DFSP was significantly lower than that in C-DFSP ( $p < 0.001$ ). Using these two immunohistochemical analyses in combination, the sensitivity and specificity for the diagnosis of FS-DFSP were 86% and 90%, respectively. Double staining of CD34 and PRAME revealed that PRAME-positive and CD34-positive areas did not overlap. This is the largest study to examine PRAME expression in FS-DFSP, and it confirmed the usefulness of PRAME in diagnosing this condition.

**Keywords** PRAME, Fibrosarcomatous dermatofibrosarcoma protuberans, QuPath, Bioimaging analysis, CD34

PRAME (PReferentially expressed Antigen in MELanoma), a member of the Cancer Testis Antigen (CTA) family, was first identified as a malignant melanoma-specific antigen<sup>1</sup> and was expected to contribute to the diagnosis and treatment of malignant melanoma. However, it was recently revealed that PRAME is actually expressed in a wide variety of malignant tumors, such as leukemia, breast cancer, and ovarian cancer<sup>2–4</sup>. Some soft tissue sarcomas (STSs) also express PRAME antigen. For example, research by Cammareri et al.<sup>5</sup> on 350 STS cases showed that STSs such as liposarcoma and angiosarcoma express PRAME antigen. They also reported that 2 out of 4 cases of fibrosarcomatous dermatofibrosarcoma protuberans (FS-DFSP) were positively stained by the PRAME antibody, although conventional dermatofibrosarcoma protuberans (C-DFSP) was negative or only very weakly positive.

FS-DFSP is the only variant of DFSP that has a significantly high potential to metastasize and thus has a remarkably worse prognosis than the other DFSP variants<sup>6</sup>. Histologically, FS-DFSP shows a characteristic herringbone pattern, a higher mitotic rate, and more severe nuclear atypia. Although almost every case of DFSP is diffusely positively stained by CD34 antibody, in FS-DFSP lesions, the positivity for CD34 is weaker. However, to date, no objectively established criterion has been approved as a threshold of CD34 positivity to differentiate FS-DFSP from C-DFSP. FS-DFSP is currently diagnosed by pathologists with extensive experience in STSs, considering the comprehensive pathological information.

In this context, PRAME positivity may be useful as a new tool for clinicians to distinguish FS-DFSP from C-DFSP. Since to the best of our knowledge no large study aimed at determining the rate of positivity of FS-DFSP to PRAME antibody has been performed, we conducted this work on 21 cases of FS-DFSP and the same number of C-DFSP cases as a control group to study this.

<sup>1</sup>Department of Anatomic Pathology, Pathological Sciences, Graduate School of Medical Sciences, Kyushu University, 3-1-1 Maidashi, Higashi-ku, Fukuoka 812-8582, Japan. <sup>2</sup>Department of Dermatology, Graduate School of Medical Sciences, Kyushu University, 3-1-1 Maidashi, Higashi-ku, Fukuoka 812-8582, Japan. <sup>3</sup>Department of Orthopaedic Surgery, Graduate School of Medical Sciences, Kyushu University, 3-1-1 Maidashi, Higashi-ku, Fukuoka 812-8582, Japan. ✉email: oda.yoshinao.389@m.kyushu-u.ac.jp

	FS-DFSP	C-DFSP
Clinical information	N=21	N=21
Age		
Mean $\pm$ SD	43.4 $\pm$ 13.5	42.4 $\pm$ 12.3
Median (range)	44 (6-66)	40 (18-65)
Sex (male/female)	13/8	12/9
Location		
Head-face-neck	1	1
Trunk	16	16
Upper extremity	1	2
Lower extremity	2	2
Viscera	1	0
Metastasis	1	0
Recurrence	2	1

**Table 1.** Clinical characteristics.

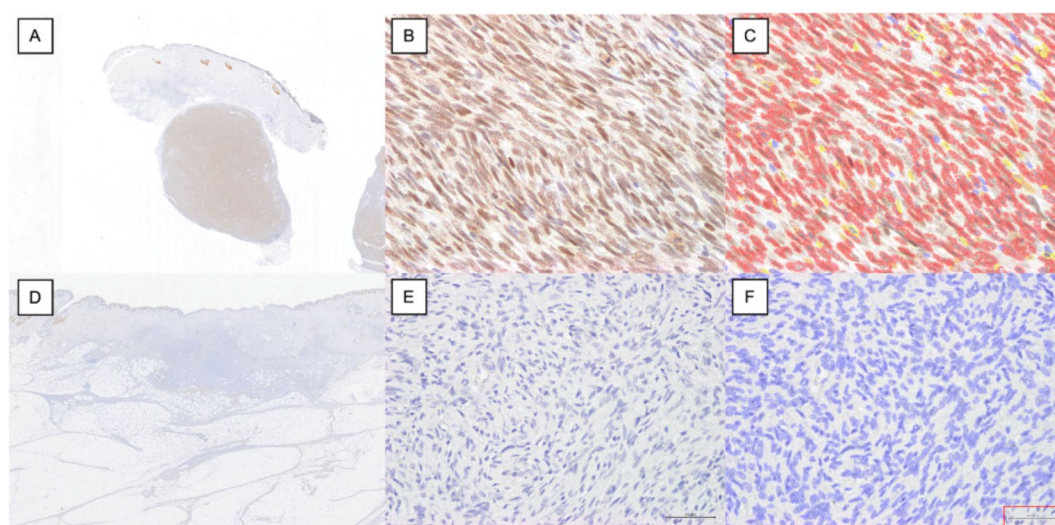


**Fig. 1.** Immunohistochemistry for PRAME in FS-DFSP and C-DFSP. A–C: FS-DFSP. A: Loupe image. The tumor is diffusely positive for PRAME. B: Magnified image ( $\times 400$ ). The tumor cells are positively stained in the nucleus. C: QuPATH processed image of B shows the staining intensity (blue: negative, yellow: weakly positive, orange: moderately positive, red: strongly positive). D–F: C-DFSP. D: Loupe image. The tumor is negative for PRAME. E: Magnified image ( $\times 400$ ). The tumor cells are negative for PRAME. F: QuPATH processed image of E shows the staining intensity (blue: negative).

## Results

### Clinicopathological data

The following clinicopathological data were collected from medical charts (Table 1).

### Immunohistochemistry

In the immunohistochemical analysis of PRAME, the staining occurred in the nucleus (Fig. 1). The average modified H-score (mH-score) was 60.9 (SD 77.1) in FS-DFSP, while it was 8.9 (SD 10.7) in C-DFSP (Fig. 2). The mH-score in FS-DFSP was significantly higher than that in C-DFSP ( $p = 0.0137$ ).

Several methods have been developed to evaluate PRAME<sup>7</sup>. Besides the H-score, a diffusely positive pattern (> 75% of the cells positive) regardless of the staining intensity is sometimes considered to represent positivity. According to this evaluation method, in the present study, 9/21 cases (43%) of FS-DFSP were positive for PRAME, while 3/21 cases (14%) of C-DFSP were positive, indicating a tendency toward a statistically significant difference between them ( $p = 0.0855$ ). Meanwhile, when we defined a focally positive pattern as reflecting positivity, 12/21 cases (57%) of FS-DFSP were positive, while 6/21 (29%) of C-DFSP were. Under this definition, there was no significant difference in PRAME positivity between FS-DFSP and C-DFSP ( $p = 0.1180$ ).

As for CD34, the staining occurred in the cytoplasmic membrane (Fig. 3). The average H-score was 79.7 (SD 42.9) in FS-DFSP, while it was 172.5 (SD 50.1) in C-DFSP (Fig. 2), which were significantly different ( $p < 0.001$ ).

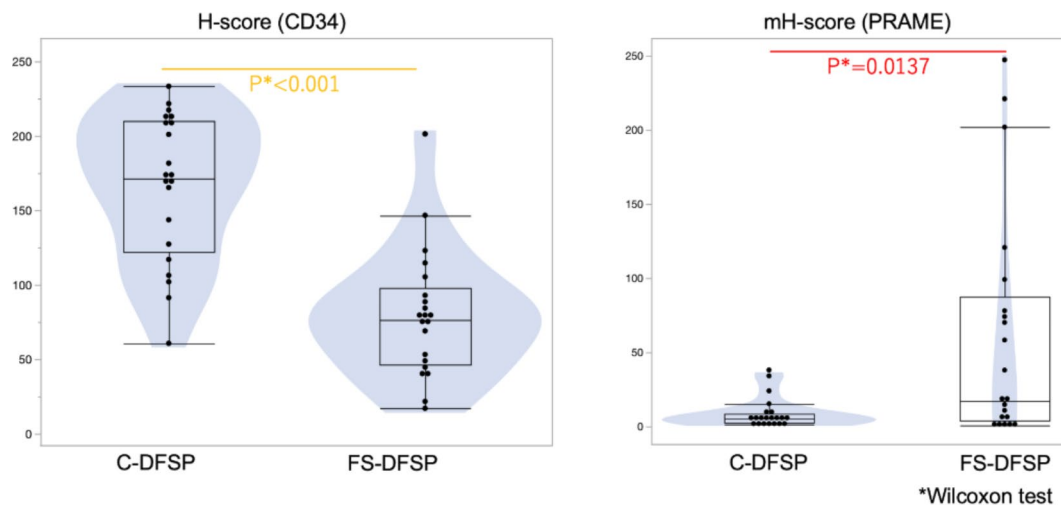


**Fig. 2.** H-score (CD34) and mH-score (PRAME) differ significantly between FS-DFSP and C-DFSP. C-DFSP shows a higher CD34 H-score and a lower PRAME mH-score, while FS-DFSP shows the opposite pattern.

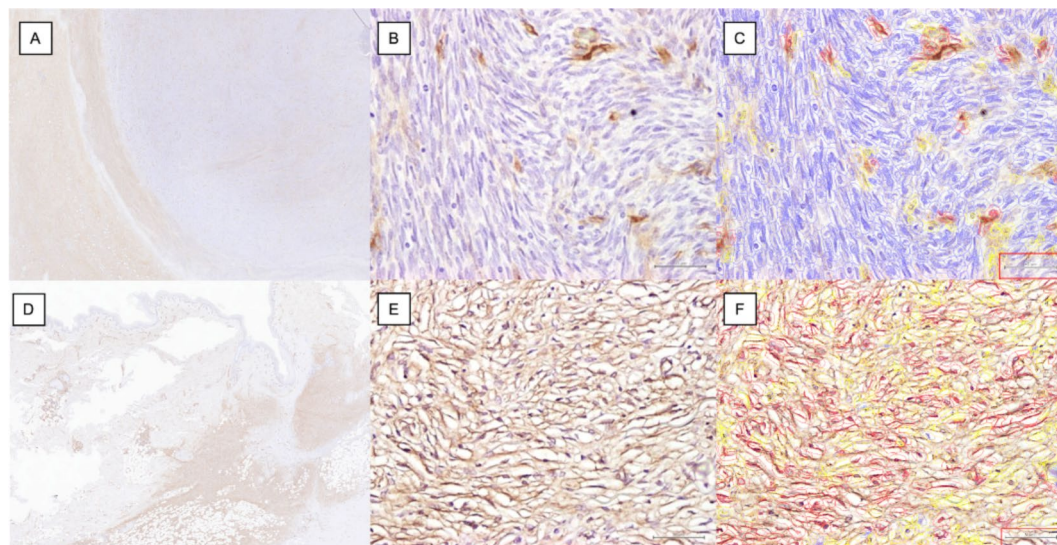


**Fig. 3.** Immunohistochemistry for CD34 in FS-DFSP and C-DFSP. A–C: FS-DFSP. A: Loupe image. The tumor cells are diffusely very weakly positive for CD34. B: Magnified image ( $\times 400$ ). The tumor cells are mostly negative for CD34. C: QuPATH processed image of B shows the staining intensity (blue: negative, yellow: weakly positive, orange: moderately positive, red: strongly positive). D–F: C-DFSP. D: Loupe image. The tumor is diffusely positive for CD34. E: Magnified image ( $\times 400$ ). The cytoplasmic membrane is diffusely positive for CD34. F: QuPATH processed image of E shows the staining intensity (blue: negative, yellow: weakly positive, orange: moderately positive, red: strongly positive).

### ROC curve

We examined the usefulness of PRAME and CD34 in the differential diagnosis of FS-DFSP and C-DFSP using the ROC curve (Fig. 4). As for PRAME, the AUC was 0.72, and the sensitivity and specificity were 67 and 81%, respectively, when the cut-off was set as an mH-score of 10.5. As for CD34, the AUC was 0.90, and the sensitivity and specificity were 76% and 95%, respectively, when the cut-off was an H-score of 90. We attempted to improve the diagnostic accuracy by combining these two antibodies. We calculated the H-score (CD34 – PRAME) (rating from  $-300$  to  $300$ ), by subtracting the mH-score (PRAME) from the H-score (CD34). The AUC in the H-score (CD34 – PRAME) was 0.92, and the sensitivity and specificity were 86% and 90%, respectively, when the cut-off was 84. We also found that the H-score (CD34) and the mH-score (PRAME) were negatively correlated ( $r = -0.33$ ,  $p = 0.03$ ) (Supplementary Fig. 1).

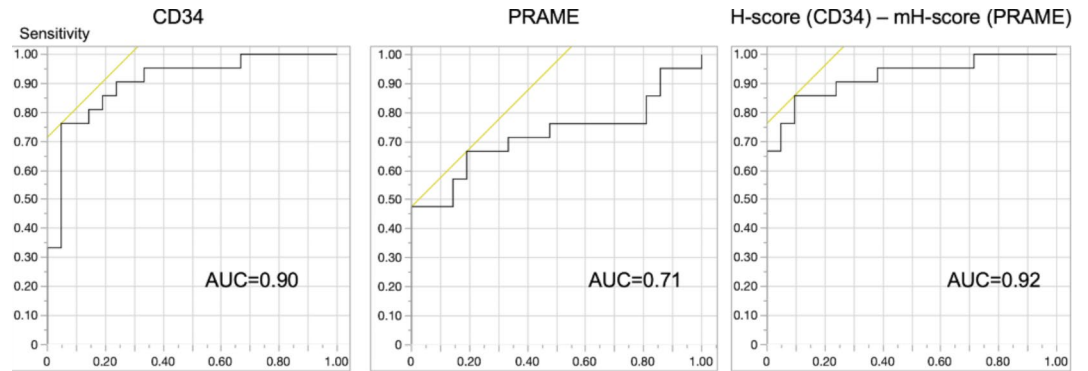


**Fig. 4.** ROC curves of H-score (CD34), mH-score (PRAME), and H-score (CD34 – PRAME). H-score (CD34 – PRAME) shows the largest AUC.

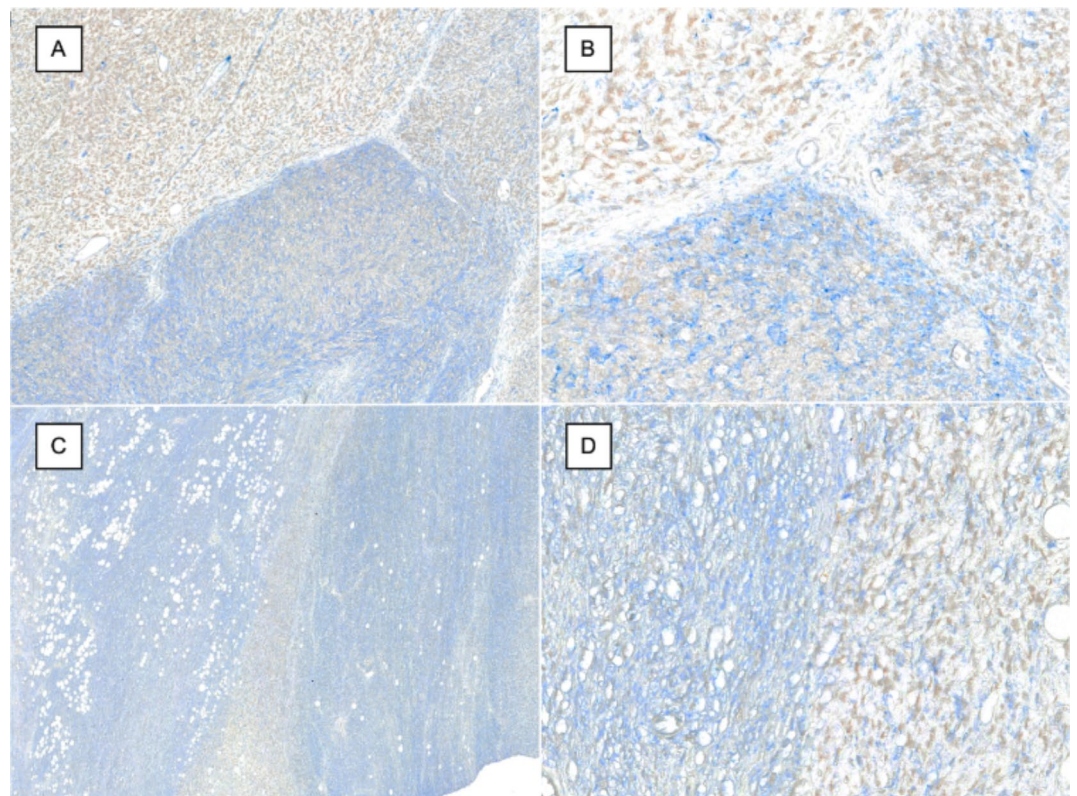


**Fig. 5.** Two cases of double staining for CD34 (blue) and PRAME (brown). A, B: Case (1) C, D: Case (2) A, C: Loupe images. The PRAME-positive areas did not overlap the CD34-positive areas. B, D: Magnified images ( $\times 400$ ). The PRAME-positive area shows decreased CD34 positivity.

### Double staining

Because we noticed that the CD34 positivity was weaker in the PRAME-positive lesions, both by visual observation and by the H-score correlation, we performed double staining of CD34 and PRAME (Fig. 5). As expected, the PRAME-positive area (brown) and the CD34-positive area (blue) did not overlap.

### Discussion

To the best of our knowledge, this is the largest study to examine PRAME expression in FS-DFSP. It was previously reported that 50% (2/4) of FS-DFSP cases exhibited at least focally positive staining for PRAME<sup>5</sup>. In the present study, we obtained findings in line with that previous report, showing that as many as 57% (12/21) of cases were focally positive. The positivity varied widely from strong, focal positivity to weak, diffuse positivity. If we set the threshold of mH-score as 10.5, 43% of the cases were judged to be positive, and the mH-score of FS-DFSP was significantly higher than that of C-DFSP ( $P=0.0137$ ). However, when we defined the positivity of PRAME by

the size of the positive area and did not take into account the staining intensity, no significant difference was observed between FS-DFSP and C-DFSP. In FS-DFSP, however, the positive area tended to be larger than in C-DFSP ( $p = 0.0855$ ), leaving the possibility that this difference may become significant in a larger study.

The findings of this study indicated that, when the H-score of CD34 is 90 or lower, there is a high likelihood of FS-DFSP. To the best of our knowledge, no previous study has compared FS-DFSP and C-DFSP by an objective semi-quantitative method using imaging analysis, so the present study is the first to attempt this. Although the specificity of CD34 in diagnosing FS-DFSP was high (95%), the sensitivity was lower (76%). In terms of diagnostic utility, PRAME did not perform better than CD34. However, H-score (CD34 – PRAME) outperformed each stain separately in terms of both sensitivity and specificity (85% and 90%, respectively). Thus, H-score (CD34 – PRAME) may thus be a useful method to diagnose FS-DFSP.

In this study, it was shown through double staining that CD34 is negative in PRAME-positive areas. PRAME is a member of the CTA family and is known to be involved in cell differentiation and proliferation through the retinoic acid (RA) pathway<sup>7</sup>. In normal tissue, PRAME is involved in gametogenesis through the maintenance of pluripotency in embryonic stem cells, particularly in the testes<sup>8</sup>. However, in various cancers such as breast cancer, non-small cell lung cancer, and uveal melanoma, PRAME expression has been shown to be associated with tumor dedifferentiation and poor prognosis<sup>3,9,10</sup>. PRAME inhibits the RA receptor pathway through SOX9, which directly activates the promoter of microphthalmia transcription factor (MITF)<sup>7</sup>. It has been demonstrated that SOX9 reduces PRAME expression<sup>11</sup>. The observed decrease in CD34 expression in PRAME-positive cells suggests that overexpression of PRAME leads to immaturity of tumor cells and a decrease in CD34 expression, which is consistent with previous reports. On the other hand, the mechanisms regulating PRAME are not fully understood. DNA hypomethylation through the transcription factors MZF1 and 5-azaC is reported to stimulate PRAME expression<sup>7</sup>, but SOX2, SOX3, and PAR signaling pathways may also be related to PRAME regulation<sup>12,13</sup>.

Recently, PRAME has garnered attention as a target for new immunotherapeutic approaches due to its tumor-specific expression<sup>1</sup>. FS-DFSP is a very rare tumor and no standardized therapy for its distant metastasis has yet been established. Imatinib, a PDGFb inhibitor, is expected to become a new agent for treating FS-DFSP, although its efficacy is still limited<sup>14</sup>. As we have shown that PRAME is significantly expressed in FS-DFSP, it could serve as a therapeutic target of these tumors as new immunotherapies emerge.

There are several limitations to this study. As mentioned above, this study is relatively small-sized, even though it is the largest of its kind. The accumulation of cases and larger-sized studies may demonstrate the significant differences between the PRAME-positive area of FS-DFSP and C-DFSP. Among the cases of FS-DFSP experienced at our institution, only 1 out of 21 cases experienced distant metastasis despite long-term follow-up. Owing to the low event rate of FS-DFSP, including local recurrence and distant metastasis, prognostic analysis could not be performed. Further studies using accumulated cases and cell lines are warranted to investigate the differences between PRAME-positive and -negative FS-DFSP. Additionally, it is important to note that the staining conditions for PRAME in this study were intentionally stronger than those for melanoma. Staining conditions for PRAME may vary slightly depending on the antibody used, and variability between facilities is expected. When staining FS-DFSP, it is necessary to establish optimal staining conditions by including melanoma (positive control) and common nevus (negative control). Finally, this study does not assert that pathologists with extensive experience of STSs are unnecessary for reaching a diagnosis. The classification of FS-DFSP in this study was based on diagnosis by such experts in our department. Furthermore, the combination of histological findings and immunohistochemistry has not been considered in this research. The objective setting of cut-offs for features such as a herringbone pattern and cellular atypia is difficult, and it is believed that the above-mentioned experts will continue to play the most important role in diagnosing FS-DFSP. However, in cases where there is difficulty in differentiating between FS-DFSP and DFSP and advice from STS experts is not available, the use of CD34 and PRAME may be helpful as an adjunct to diagnosis.

## Methods

### Materials

Samples from 68 cases between 2004 and 2023 that were previously diagnosed as DFSP were retrieved from the soft tissue tumors registered in the files of the Department of Anatomic Pathology, Pathological Sciences, Graduate School of Medical Sciences, Kyushu University, Fukuoka, Japan. Among them, 21 cases with fibrosarcomatous (FS) lesions were enrolled in this study, while we also collected 21 cases of age/sex/location-matched DFSP as a control group.

### Immunohistochemistry

From formalin-fixed, paraffin-embedded blocks, a single representative block was chosen for each case for immunohistochemistry (IHC) and was sectioned at 3  $\mu$ m thickness. H&E staining and IHC staining for CD34 (QEnd10; Dako, Glostrup, Denmark) and PRAME (ER20330; Abcam, Cambridge, UK) were performed. The primary antibodies, their dilutions, and the antigen retrieval are summarized in Supplementary Table 1. As positive and negative controls for PRAME, malignant melanoma cases and common nevus cases were selected, respectively. The immune complexes were detected with the DAKO EnVision Detection System (Dako).

We then performed double immunostaining of PRAME and CD34. In addition to the immunodetection using the horseradish peroxidase method mentioned above, N-Histofine Simple Stain AP (Nichirei Biosciences Inc., Tokyo, Japan) and PermaBlue Plus (Diagnostic BioSystems Inc., Pleasanton, CA) were used as the secondary antibody and the chromogen, respectively.

## H-scoring and imaging analysis

IHC for CD34 was semi-quantitatively evaluated, using the H-score. In each high-power field (HPF) ( $\times 400$ ), the positivity of each cell was classified into the following four classes: negative: 0, weakly positive: 1, moderately positive: 2, and strongly positive: 3. We obtained the H-score (0–300) by multiplying the proportion (%) of stained cells by the staining intensity (0–3). We selected three random fields from the tumor lesion and calculated the average of their H-scores as the final H-score. We used QuPath ver. 5.1<sup>15</sup>, an open-source platform, for bioimaging analysis. We created projects by importing JPEG images of the HPFs and performed positive cell detection to recognize the proportion and intensity of the IHC. The nuclear parameters were set as follows: nuclear size of 150 to 2000 pixels<sup>2</sup>, cell expansion of 20 pixels, and background radius of 40 pixels. We did not split the image by shape. As for the intensity threshold parameters, we evaluated the maximum staining in the cytoplasm and divided it into three threshold levels: weak (+1, highlighted in yellow), moderate (+2, orange), and strong (+3, red). Negatively stained cells were highlighted in blue. QuPath software automatically provided us with an H-score.

As for the evaluation of IHC for PRAME, because the staining intensity varied markedly within a tumor lesion, we could not obtain an H-score by simply averaging HPFs from random areas. Therefore, we classified the whole slides into four areas (negative, weakly positive, moderately positive, strongly positive) via observations at low magnification ( $\times 100$ ), and calculated the percentage of each area among the whole slide (area; %). Then, we obtained the H-score/HPF for each area, in the same way as for CD34, using QuPath. As for the intensity threshold parameters, we evaluated the maximum staining in the nucleus. We calculated the final modified H-score (mH-score) by summing up the scores of the percentage of each area multiplied by the H-score/HPF of the area [negative area (%)  $\times$  H-score/HPF (negative) + weakly positive area (%)  $\times$  H-score/HPF (weakly positive) + moderately positive area (%)  $\times$  H-score/HPF (moderately positive) + strongly positive area (%)  $\times$  H-score/HPF (strongly positive)] (Supplementary Table 2).

## Statistical analysis

We statistically analyzed the obtained H-score and mH-score using the Wilcoxon single-rank test in the statistical analytical software JMP (ver. 17.0.0) (Supplementary Table 3). A two-sided p-value of  $< 0.05$  was considered to be statistically significant. To evaluate the diagnostic performance of PRAME and CD34 in distinguishing FS-DFSP from C-DFSP, we employed the Receiver Operating Characteristic (ROC) curve analysis and the Area Under the Curve (AUC), using JMP. The curve was created by plotting the true positive rate (sensitivity) against the false positive rate (1-specificity) at various threshold settings. An AUC value of 1.0 represents perfect accuracy, while an AUC of 0.5 indicates no diagnostic ability.

## Data availability

All data generated and analyzed in this study are provided within the manuscript or supplementary information files.

Received: 16 April 2024; Accepted: 26 September 2024

Published online: 03 October 2024

## References

- Al-Khadairi, G. & Decock, J. Cancer testis antigens and immunotherapy: where do we stand in the targeting of PRAME? *Cancers (Basel)*. **11**, 984 (2019).
- Ding, K. et al. PRAME gene expression in acute leukemia and its clinical significance. *Cancer Biol. Med.* **9**, 73–76 (2012).
- Doolan, P. et al. Prevalence and prognostic and predictive relevance of PRAME in breast cancer. *Breast Cancer Res. Treat.* **109**, 359–365 (2008).
- Šafanda, A. et al. Immunohistochemical expression of PRAME in 485 cases of epithelial tubo-ovarian tumors. *Virchows Arch.* **483**, 509–516 (2023).
- Cammareri, C. et al. PRAME immunohistochemistry in soft tissue tumors and mimics: a study of 350 cases highlighting its imperfect specificity but potentially useful diagnostic applications. *Virchows Arch.* **483**, 145–156 (2023).
- Abbott, J. J., Oliveira, A. M. & Nascimento, A. G. The prognostic significance of fibrosarcomatous transformation in dermatofibrosarcoma protuberans. *Am. J. Surg. Pathol.* **30**, 436–443 (2006).
- Cassalia, F. et al. PRAME updated: Diagnostic, prognostic, and therapeutic role in skin cancer. *Int. J. Mol. Sci.* **25**, 1582 (2024).
- Kern, C. H., Yang, M. & Liu, W. S. The PRAME family of cancer testis antigens is essential for germline development and gametogenesis. *Biol. Reprod.* **105**, 290–304 (2021).
- Szczepanski, M. J. et al. PRAME expression in head and neck cancer correlates with markers of poor prognosis and might help in selecting candidates for retinoid chemoprevention in pre-malignant lesions. *Oral Oncol.* **49**, 144–151 (2013).
- Broggi, G. et al. Immunohistochemical expression of PRAME is a marker of poor prognosis in uveal melanoma: a clinicopathologic and immunohistochemical study on a series of 85 cases. *Pathol. Res. Pract.* **247**, 154543 (2023).
- Passeron, T. et al. Upregulation of SOX9 inhibits the growth of human and mouse melanomas and restores their sensitivity to retinoic acid. *J. Clin. Invest.* **119**, 954–963 (2009).
- Lee, Y. K. et al. Tumor antigen PRAME is up-regulated by MZF1 in cooperation with DNA hypomethylation in melanoma cells. *Cancer Lett.* **403**, 144–151 (2017).
- Epping, M. T. et al. The human tumor antigen PRAME is a dominant repressor of retinoic acid receptor signaling. *Cell.* **122**, 835–847 (2005).
- Rutkowski, P. et al. Long-term results of treatment of advanced dermatofibrosarcoma protuberans (DFSP) with imatinib mesylate - the impact of fibrosarcomatous transformation. *Eur. J. Surg. Oncol.* **43**, 1134–1141 (2017).
- Bankhead, P. et al. QuPath: open source software for digital pathology image analysis. *Sci. Rep.* **7**, 16878 (2017).

## Acknowledgements

This work was supported by JSPS KAKENHI Grant Number 19H03444.

### Author contributions

T. Ichiki performed the research and wrote the paper. T. Ito contributed to the research design and slide review. S. S. and Y. N. contributed to the acquisition of the samples. T. N. and Y. O. designed the research and gave final approval of the manuscript. All authors critically reviewed and approved the manuscript.

### Funding

The authors declare that there are no sources of external funding.

### Declarations

#### Compliance with ethical standards

This study was conducted in accordance with the principles embodied in the Declaration of Helsinki. This study was also approved by the Ethics Committee of Kyushu University (Nos. 29–625, 29–429, 2020 – 361, 2021 – 165). Written informed consent was obtained from each patient before his/her enrollment to the research.

#### Competing interests

The authors declare that they have no significant relationships with, or financial interest in, any commercial entities pertaining to this article.

#### Additional information

**Supplementary Information** The online version contains supplementary material available at <https://doi.org/10.1038/s41598-024-74556-5>.

**Correspondence** and requests for materials should be addressed to Y.O.

**Reprints and permissions information** is available at [www.nature.com/reprints](http://www.nature.com/reprints).

**Publisher's note** Springer Nature remains neutral with regard to jurisdictional claims in published maps and institutional affiliations.

**Open Access** This article is licensed under a Creative Commons Attribution-NonCommercial-NoDerivatives 4.0 International License, which permits any non-commercial use, sharing, distribution and reproduction in any medium or format, as long as you give appropriate credit to the original author(s) and the source, provide a link to the Creative Commons licence, and indicate if you modified the licensed material. You do not have permission under this licence to share adapted material derived from this article or parts of it. The images or other third party material in this article are included in the article's Creative Commons licence, unless indicated otherwise in a credit line to the material. If material is not included in the article's Creative Commons licence and your intended use is not permitted by statutory regulation or exceeds the permitted use, you will need to obtain permission directly from the copyright holder. To view a copy of this licence, visit <http://creativecommons.org/licenses/by-nc-nd/4.0/>.

© The Author(s) 2024